International Scholarly Research Network
ISRN Nanomaterials
Volume 2012, Article ID 769528, 7 pages
doi:10.5402/2012/769528

Research Article

Synthesis and Characterization of Nanometric Pure Phase SnO_2 Obtained from Pyrolysis of Diorganotin(IV) Derivatives of Macrocycles

Mala Nath and P. K. Saini

Department of Chemistry, Indian Institute of Technology, Roorkee 247667, India

Correspondence should be addressed to Mala Nath, malanfcy@iitr.ernet.in

Received 11 July 2012; Accepted 27 July 2012

Academic Editors: W. Bao and A. Fidalgo

Thermal decomposition of diorganotin(IV) derivatives of macrocycles of general formula, $R_2Sn(L1)$ and $R_2Sn(L2)$ (where R = *n*-butyl (**1/4**), methyl (**2/5**), and phenyl (**3/6**); H_2L1 = 5,12-dioxa-7,14-dimethyl-1,4,8,11-tetraazacyclotetradeca-1,8-diene and H_2L2 = 6,14-dioxa-8,16-dimethyl-1,5,9,13-tetraazacyclotetradeca-1,9-diene), provides a simple route to prepare nanometric SnO_2 particles. X-ray line broadening shows that the particle size varies in the range of 36–57 nm. The particle size of SnO_2 obtained by pyrolysis of **3** and **5** is in the range of ~5–20 nm as determined by transmission electron microscope (TEM). The surface morphology of SnO_2 particles was determined by scanning electron microscopy (SEM). Mathematical analysis of thermogravimetric analysis (TGA) data shows that the first step of decomposition of compound **4** follows first-order kinetics. The energy of activation (E^*), preexponential factor (A), entropy of activation (S^*), free energy of activation (G^*), and enthalpy of activation (H^*) of the first step of decomposition have also been calculated. $Me_2Sn(L2)$ and $Ph_2Sn(L1)$ are the best precursors among the studied diorganotin(IV) derivatives of macrocycles for the production of nanometric SnO_2.

1. Introduction

In recent years nanometric SnO_2 is of current interest because of its semiconducting, optical, and electronic properties. In addition to these, tin(IV) oxide possesses potential applications such as catalytic supports [1, 2], transparent conducting electrodes [3], and gas sensors [4, 5]. SnO_2 is preferred over other metal oxides in gas sensors because of its high sensitivity and selectivity for different gases (e.g., H_2) in mixture [6]. Nanometric SnO_2 has different properties from bulk crystals; therefore, much attention has been addressed to synthesis and characterization of such materials. To produce nanometric SnO_2, a variety of chemical and physical methods [7–11] have been reported in the literature.

Tetraazamacrocycles and their derivatives have drawn special attention because of their applications in various fields such as analytical, industry, medicinal, and biological [12–16]. A thorough survey of literature reveals that only a few attempts have been made to study the thermal stability of metal complexes of tetraazamacrocycles [17]. However, a considerable attention has been given to the thermal decomposition of organometallic compounds in the last few years because they decompose at low temperature producing metallic oxides/sulfides and metallic particles. A thorough survey of literature reveals that limited studies have been carried out to prepare nanometric SnO_2 by the pyrolysis of single source organotin precursors [18–20]. Further, it is important to mention that there is only a single reference recently reported by us in which some organotin-macrocyclic complexes are used as single source precursors for preparation of nanometric SnO_2 through their pyrolysis route [21]. It is, therefore, worth investigating to explore the best precursors which would produce pure phase, nanosized SnO_2 on thermal decomposition.

In the present study, we report herein a simple route to prepare SnO_2 semiconducting nanoparticles by the thermal decomposition of diorganotin(IV) derivatives of 5,12-dioxa-7,14-dimethyl-1,4,8,11-tetraazacyclotetradeca-1,8-diene and

6,14-dioxa-8,16-dimethyl-1,5,9,13-tetraazacyclotetradeca-1, 9-diene using thermogravimetric analysis (TGA) and differential thermal analysis (DTA) techniques under air atmosphere. The residues (SnO_2) obtained were characterized by infrared (IR), X-ray diffraction analysis (XRD), scanning electron microscopy (SEM), field emission scanning electron microscopy in combination with energy-dispersive X-ray spectrometry (FESEM-EDX), and transmission electron microscopy with electron diffraction analysis (TEM-ED).

2. Experimental Section

The details of synthesis and characterization of these organotin(IV)-macrocyclic complexes are similar to those reported previously [22]. Thermal measurements thermogravimetric (TG), differential thermal analysis (DTA) and derivative thermogravimetric (DTG), infrared (IR), and X-ray diffraction pattern (XRD) of residues were recorded on the same instruments as reported previously [22]. Nanometric SnO_2 was prepared by the thermal decomposition of organotin(IV) precursors in a tube furnace under similar experimental conditions up to the formation temperature of SnO_2 as determined by TG analysis. The surface morphology of SnO_2 particles was studied by using scanning electron microscope (SEM) and FESEM-EDX. The SEM images were recorded on a LEO 435 VP electron microscope and FESEM-EDX on FEI Quanta 200 FEG. The transmission electron photographs of SnO_2 particles obtained from Ph_2Sn(L1) and Me_2Sn(L2) were recorded on a FEI TECNAI 20 G2STWIN, at Institute Instrumentation Center, Indian Institute of Technology Roorkee, Roorkee. To record the SEM and FESEM with EDX analysis, SnO_2 particles were previously agitated ultrasonically for 30 min in dichloromethane to separate out nanoparticles from the algometric form. After agitation, the sample was placed on the glass slit with the help of a capillary, which was made conducting by silver gel and after drying the solvent, the sample was covered with gold thin layer. For TEM studies, the agitated particles under suspension were taken on the carbon grid. After drying the sample the TEM photographs were taken and recorded.

3. Results and Discussion

The structure and stoichiometry of the single source precursors, namely, orgaotin(IV) derivatives of macrocycles of general formula, R_2Sn(L1) and R_2Sn(L2) (where R = *n*-butyl, methyl, and phenyl; H_2L1 = 5,12-dioxa-7,14-dimethyl-1,4,8,11-tetraazacyclotetra-deca-1,8-diene and H_2L2 = 6,14-dioxa-8,16-dimethyl-1,5,9,13-tetraazacyclotetradeca-1, 9-diene) were established by the various physicochemical and spectral studies as reported in our previous communication [22], and are again represented in Figures 1(a) and 1(b).

The TG and DTA curves of these compounds are presented in Figures 2 and 3, respectively, and the XRD patterns of the residues obtained are presented in Figure 4. As reported [22] earlier all of these complexes, except

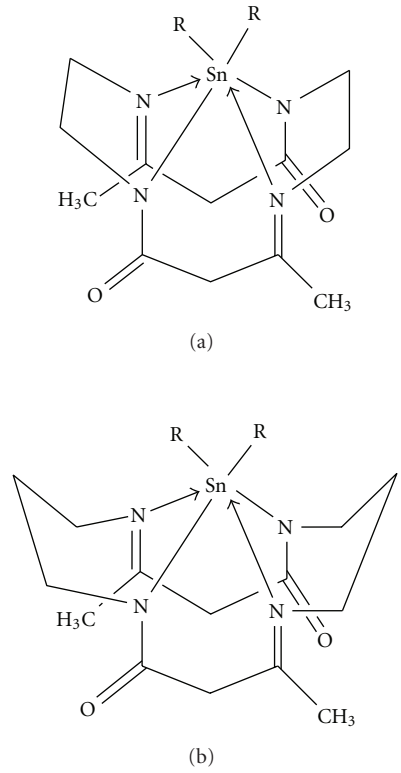

Figure 1: Structure of organotin(IV) macrocycles [22].

n-Bu_2Sn(L2), decomposed in two or three steps in the temperature range 100–1000°C yielding SnO_2 in the temperature range 252–600°C, which was confirmed by the XRD analysis and by the presence of ν(Sn–O) at 620 ± 5 cm^{-1}.

The crystallite average size calculated by Scherrer equation [19, 23] (1) is in the range of 36−57 nm (Table 1).

$$D = \frac{\lambda}{\Delta W(\cos\theta)}, \tag{1}$$

where λ = 1.5418 Å is the wavelength of the incident beam, ΔW is the full width at half maximum in radians of the highest intensity line, and θ is the Bragge's angle.

The SEM image of the residue (SnO_2) obtained by thermal decomposition of *n*-Bu_2Sn(L1) at 500–525°C is shown in Figure 5. The residues obtained by the pyrolysis of diorganotin(IV) derivatives of macrocycles were agitated ultrasonically for 30 min. In all the cases the SEM images of the residues (SnO_2) showed uniform grain size with almost spherical shape. The grain size measured by SEM is in the range of ~20–200 nm in diameter. FESEM image with EDX analysis of the residue obtained by pyrolysis of Me_2Sn(L2) is represented in Figure 6. These images depict the formation of almost spherical particles in all of the cases. EDX analyses of these particles in SEM micrographs at various locations marked with the sign "+" show them to consist of Sn and O with SnO_2 composition.

The size of SnO_2 particles obtained by pyrolysis of Ph_2Sn(L1) and Me_2Sn(L2) measured by TEM is in the range

Table 1: Comparison of average size of the SnO_2 particles obtained by XRD, SEM, and TEM.

SnO_2 particles obtained from precursors	Particles size by XRD (nm)	Particles size by SEM (nm)	Particles size by TEM (nm)
n-Bu_2Sn (L1)	41.68	50–200	—
Me_2Sn (L1)	57.26	50–145	—
Ph_2Sn (L1)	37.26	20–120	5–20
n-Bu_2Sn (L2)	41.69	50–180	—
Me_2Sn (L2)	35.81	20–100	5–15
Ph_2Sn (L2)	41.69	20–150	—

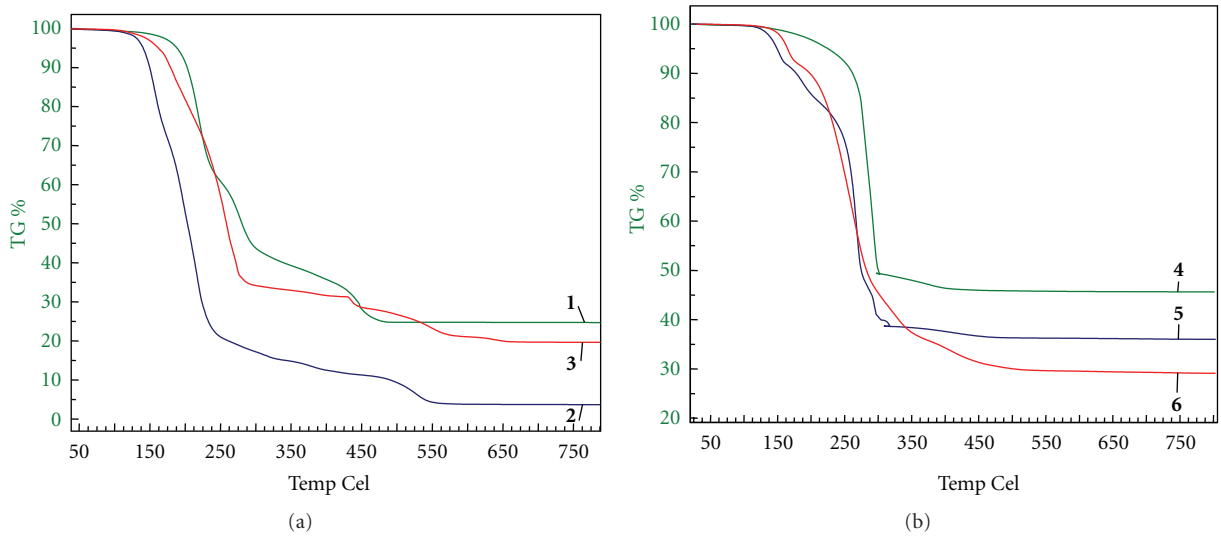

Figure 2: TGA plots of *n*-Bu_2Sn(L1) (**1**), Me_2Sn(L1) (**2**), Ph_2Sn(L1) (**3**), *n*-Bu_2Sn(L2) (**4**), Me_2Sn(L2) (**5**), and Ph_2Sn(L2) (**6**).

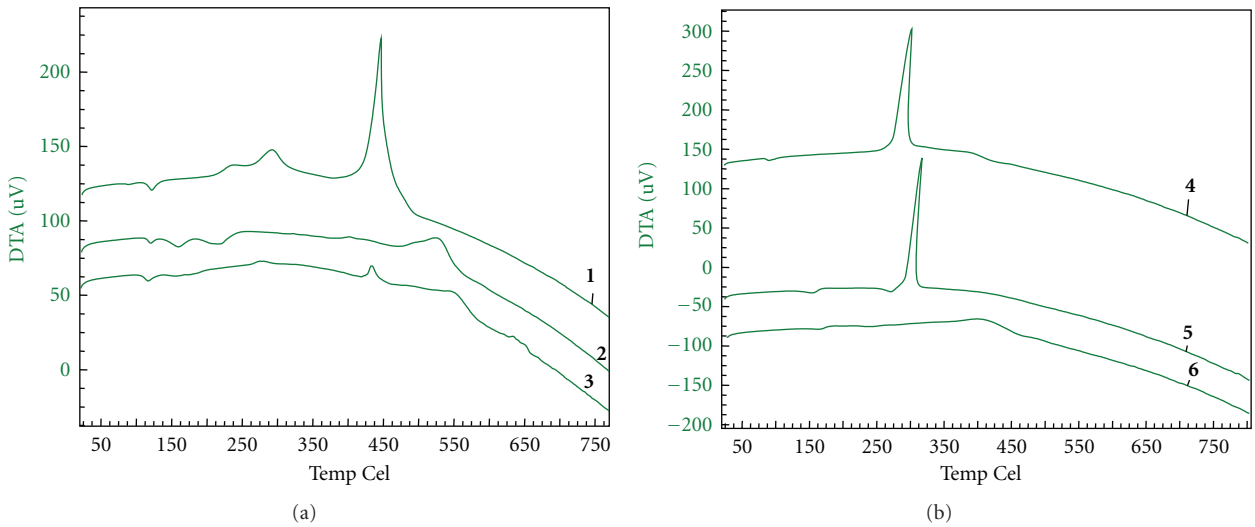

Figure 3: DTA plots of *n*-Bu_2Sn(L1) (**1**), Me_2Sn(L1) (**2**), Ph_2Sn(L1) (**3**), *n*-Bu_2Sn(L2) (**4**), Me_2Sn(L2) (**5**), and Ph_2Sn(L2) (**6**).

of ~5–20 nm (Figures 7 and 8). There are many particles and holes about 5–20 nm size. Many connected grains form a random net work, in which various nanosized holes appear (Figure 8). Such structure is named as nanosponge [1]. This microstructure leads to a very high rate of interface and surface. There are a large number of nanometric grains in Figure 7, which have well-ordered lattices. The electron diffraction pattern of selected area (inset in Figures 7 and 8) appeared to be typical polycrystalline diffraction rings. According to the diameters of the rings, the spacings are 0.34,

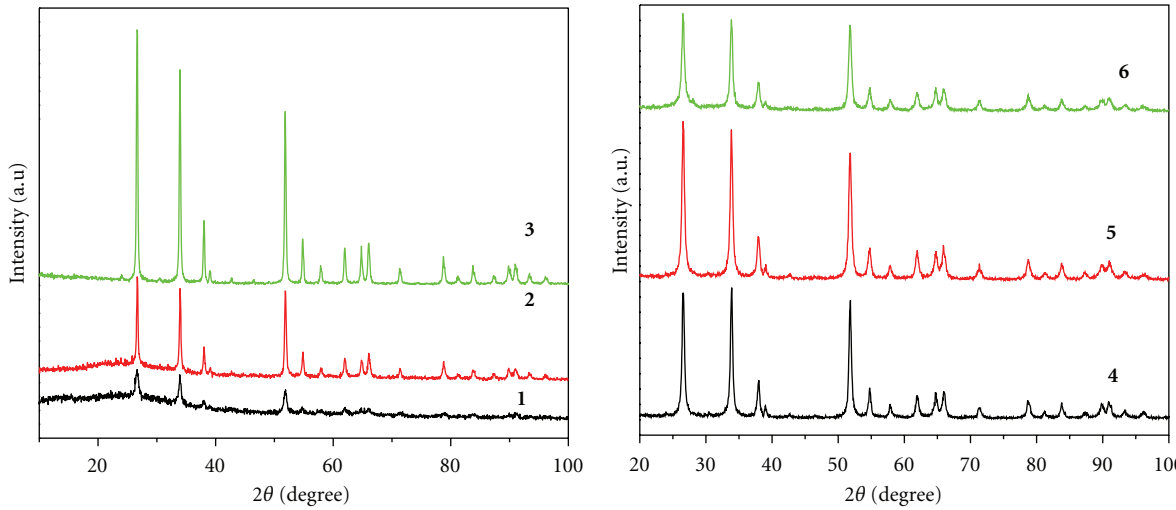

Figure 4: X-ray diffraction of SnO_2 obtained from pyrolysis of (a) n-Bu_2Sn(L1) (**1**), Me_2Sn(L1) (**2**), Ph_2Sn(L1) (**3**); (b) n-Bu_2Sn(L2) (**4**), Me_2Sn(L2) (**5**), Ph_2Sn(L2) (**6**).

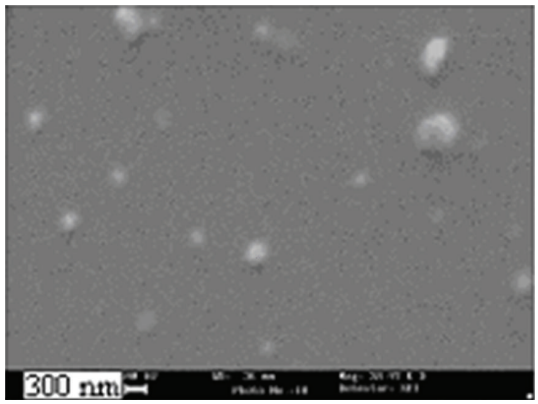

Figure 5: SEM image of SnO_2 particles obtained by pyrolysis of n-Bu_2Sn(L1).

0.026, 0.024 nm and 0.33, 0.026, 0.024 nm for SnO_2 particles obtained by pyrolysis of Ph_2Sn(L1) and Me_2Sn(L2), respectively. They are in accordance with the spacing of [110], [101], and [200] of tetragonal phase SnO_2. This indicates that the grains are nanocrystalline tetragonal SnO_2 [5]. On the basis of the above studies, Me_2Sn(L2) and Ph_2Sn(L1) are the best precursors among the studied diorganotin(IV) derivatives of macrocycles for the production of nanometric SnO_2.

TG curves of n-Bu_2Sn(L2) show that the first step of the complex exhibits a characteristic, well-defined, and nonoverlapping pattern. Two different methods were used to evaluate kinetic data from the TG traces. The following kinetic data are applicable only for the first step of decomposition of the complexes, as the other steps are very slow and do not follow the first-order kinetics; therefore, kinetic parameters for those steps have not been evaluated. The order of decomposition of the n-Bu_2Sn(L2) complex is obtained by using Horowitz and Metzger equation [24]. The value of Cs is 0.391. Therefore, the calculated order shows that the decomposition follows first-order kinetics. The values of energy of activation (E^*) and preexponential factor (A) have been calculated using two different methods, namely, Horowitz and Metzger [24] and Coats and Redfern [25] methods. Following equations were employed to calculate the entropy of activation (2), the enthalpy of activation (3), and free energy of activation (4):

$$S^* = 2.303\left(\log\frac{Ah}{kT}\right)R, \tag{2}$$

$$H^* = E^* - RT, \tag{3}$$

$$G^* = H^* - TS^*, \tag{4}$$

where h and k are the Planck's and Boltzmann constants, respectively.

Kinetic parameters are given in Table 2. The negative values of S^* indicate that the decomposition reaction is slow. The plot of Horowitz and Metzger method of n-Bu_2Sn(L2) (**4**) is presented in Figure 9(a), whereas that of Coats and Redfern method is presented in Figure 9(b).

4. Conclusions

The residues obtained from thermal decomposition of R_2Sn(L1) and R_2Sn(L2) are SnO_2 as confirmed previously [22] by XRD analysis and infrared spectral studies. The crystal average size of SnO_2 calculated by Scherrer equation is in the range of 36–57 nm, whereas the size measured by

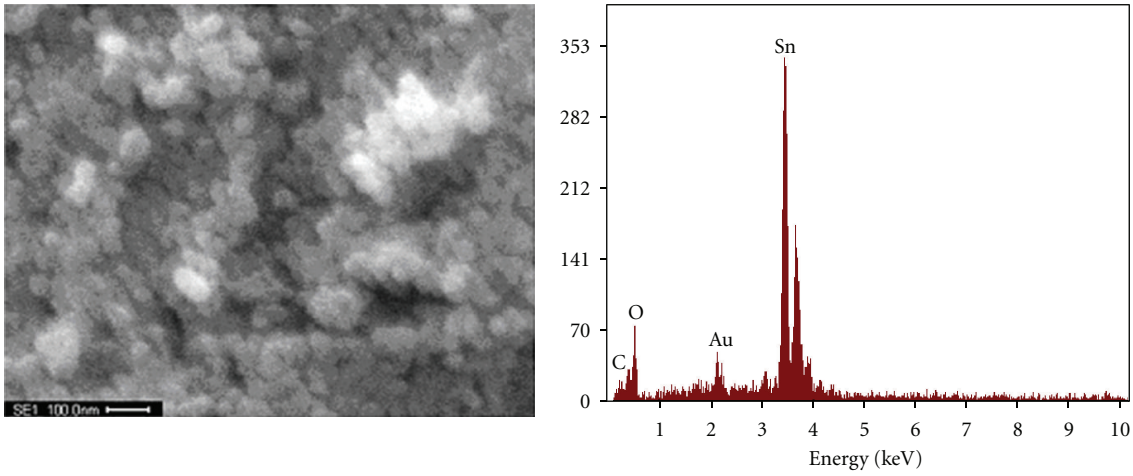

(a) (b)

Figure 6: FESEM image with EDX of SnO_2 particles obtained by pyrolysis of Me_2Sn(L2).

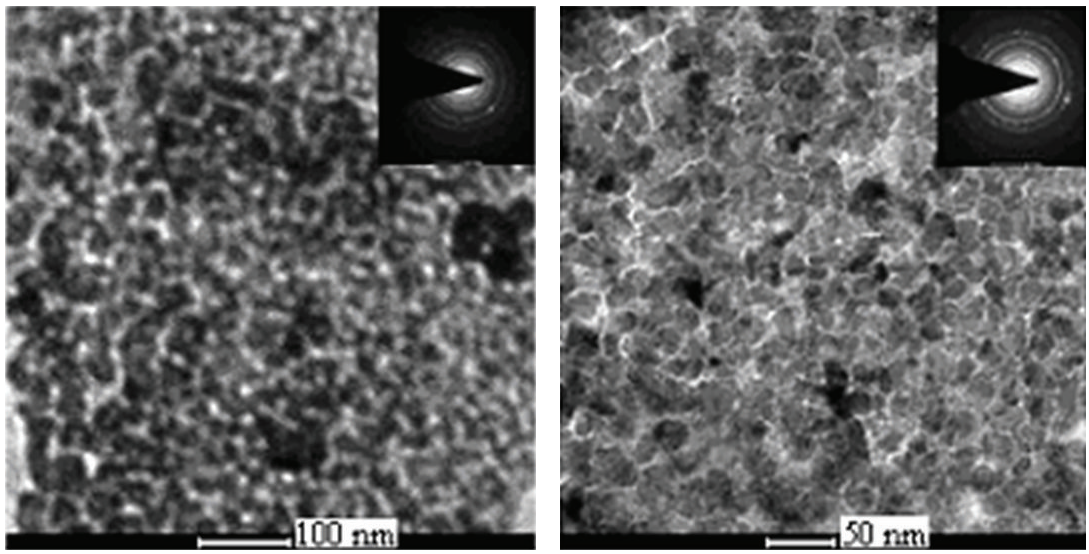

(a) (b)

Figure 7: TEM images of SnO_2 particles obtained by pyrolysis of Ph_2Sn(L1) with electron diffraction pattern.

Table 2: Kinetic data of thermal decomposition of n-Bu_2Sn (L2).

Complex	Parameters	From Horowitz and Metzger method	From Coats and Redfern method
n-Bu_2Sn (L2)	E^* (kJ mol^{-1})	272.20	312.67
	A (s^{-1})	9.01×10^{23}	7.2×10^{24}
	S^* (J K^{-1} mol^{-1})	−672.31	−655.00
	G^* (kJ mol^{-1})	644.70	680.13
	H^*(kJ mol^{-1})	267.53	312.67

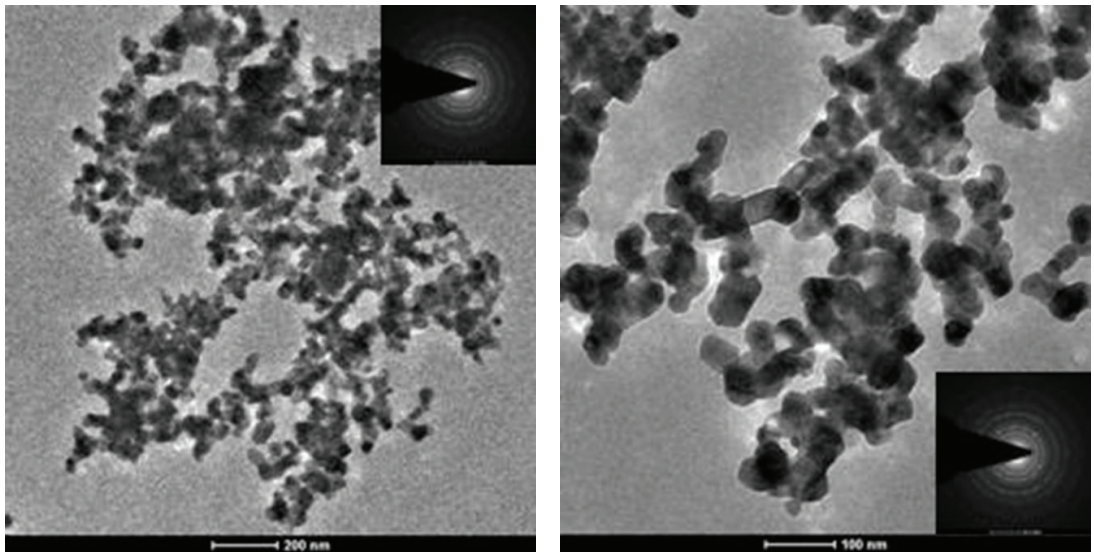

(a) (b)

Figure 8: TEM images of SnO_2 particles obtained by pyrolysis of Me_2Sn(L2) with electron diffraction pattern.

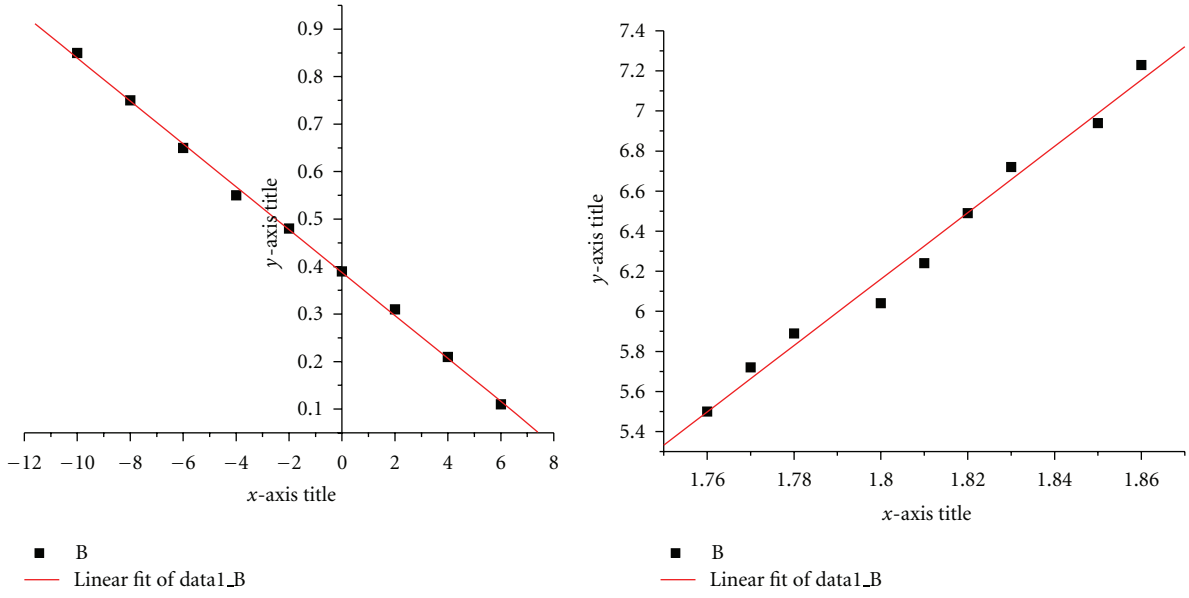

(a) (b)

Figure 9: For n-Bu_2Sn(L2) (a) a plot of $[-\log(\log(W_\infty/W_r)]$ versus θ $(T - T_s)$ (K) (Horowitz and Metzger method); and (b) a plot of $[-\log(\ln(W_\infty/W_r)/T^2]$ versus $(1/T) \times 10^{-3}$ K (Coats and Redfern method).

SEM and TEM is in the range of ~20–200 nm and ~5–20 nm, respectively, in diameter. Me_2Sn(L2) and Ph_2Sn(L1) are the best precursors among the studied diorganotin(IV) derivatives of macrocycles for the production of nanosized tetragonal SnO_2. The kinetic parameters of the first-step decomposition of n-Bu_2Sn(L2) indicate that its decomposition is slow.

Acknowledgments

The authors are thankful to the Head, Institute Instrumentation Centre, Indian Institute of Technology Roorkee, Roorkee, India, for providing facilities to carry out thermal studies, X-ray diffraction analysis and to record SEM, FESEM-EDX, and TEM-ED images. Mr. P. K. Saini is thankful to the Council of Scientific and Industrial Research, New Delhi, India, for awarding Senior Research Fellowship.

References

[1] W. Dazhi, W. Shulin, C. Jun, Z. Suyuan, and L. Fangqing, "Microstructure of SnO_2," *Physical Review B*, vol. 49, no. 20, pp. 14282–14285, 1994.

[2] D. E. Williams and K. F. E. Pratt, "Classification of reactive sites on the surface of polycrystalline tin dioxide," *Journal of*

the Chemical Society, Faraday Transactions, vol. 94, pp. 3493–3500, 1998.

[3] T. El Moustafid, H. Cachet, B. Tribollet, and D. Festy, "Modified transparent SnO_2 electrodes as efficient and stable cathodes for oxygen reduction," *Electrochimica Acta*, vol. 47, no. 8, pp. 1209–1215, 2002.

[4] A. R. Phani, S. Manorama, and V. J. Rao, "Preparation, characterization and electrical properties of SnO_2 based liquid petroleum gas sensor," *Materials Chemistry and Physics*, vol. 58, no. 2, pp. 101–108, 1999.

[5] G. J. Li, X. H. Zhang, and S. Kawi, "Relationships between sensitivity, catalytic activity, and surface areas of SnO_2 gas sensors," *Sensors and Actuators B*, vol. 60, no. 1, pp. 64–70, 1999.

[6] M. Batzill and U. Diebold, "The surface and materials science of tin oxide," *Progress in Surface Science*, vol. 79, no. 2–4, pp. 47–154, 2005.

[7] C. H. Shek, J. K. C. Lai, and G. M. Lin, "Grain growth in nanocrystalline SnO_2 prepared by sol-gel route," *Nanostructured Materials*, vol. 11, no. 7, pp. 887–893, 1999.

[8] T. Wang, Z. N. X. F. Ma, and Z. Y. Jiang, "The one-step preparation and electrochemical characteristics of tin dioxide nanocrystalline materials," *Electrochemistry Communications*, vol. 5, no. 7, pp. 599–602, 2003.

[9] Y. D. Wang, C. L. Ma, X. D. Sun, and H. D. Li, "Preparation and characterization of SnO_2 nanoparticles with a surfactant-mediated method," *Nanotechnology*, vol. 13, no. 5, article 565, 2002.

[10] U. Kersen, "The gas-sensing potential of nanocrystalline SnO_2 produced by a mechanochemical milling via centrifugal action," *Physics and Astronomy*, vol. 75, no. 5, pp. 559–563, 2002.

[11] R. D. Tarey and T. A. Raju, "A method for the deposition of transparent conducting thin films of tin oxide," *Thin Solid Films*, vol. 128, no. 3-4, pp. 181–189, 1985.

[12] K. Y. Choi, M. J. Kim, D. S. Kim et al., "Preparation and characterization of Nickel(II) and Copper(II) tetaaza macrocyclic complexes with isonicotinate ligands," *Bulletin of the Korean Chemical Society*, vol. 23, no. 8, pp. 1062–1066, 2002.

[13] P. V. Bernhardt, J. C. Hetherington, and L. A. Jones, "N-Methylation of diamino-substituted macrocyclic complexes: intramolecular cyclisation," *Journal of the Chemical Society—Dalton Transactions*, no. 23, pp. 4325–4330, 1996.

[14] E. Kimura, "Macrocyclic polyamine Zinc(II) complexes as advanced models for Zinc(II) enzymes," *Progress in Inorganic Chemistry*, vol. 41, p. 443, 1994.

[15] K. Kumar and M. F. Tweedle, "Ligand basicity and rigidity control formation of macrocyclic polyamino carboxylate complexes of gadolinium(III)," *Inorganic Chemistry*, vol. 32, pp. 4193–4199, 1993.

[16] A. Bansal and R. V. Singh, "Template synthesis, structural and biological studies of new tetraazamacrocyclic complexes of lead(II)," *Boletín de la Sociedad Chilena de Química*, vol. 45, no. 3, p. 479, 2000.

[17] M. Shakir, H. T. N. Chishti, and P. Chingsubam, "Metal ion-directed synthesis of 16-membered tetraazamacrocyclic complexes and their physico-chemical studies," *Spectrochimica Acta A*, vol. 64, no. 2, pp. 512–517, 2006.

[18] M. Nath, S. Goyal, G. Eng, and D. Whalen, "Synthesis, spectral, thermal, and biological studies of adducts of organotin(IV) halides with Schiff bases derived from 2-amino-5-(*o*-methoxyphenyl)-1,3,4-thiadiazole ," *Bulletin of the Chemical Society of Japan*, vol. 69, no. 3, pp. 605–612, 1996.

[19] A. G. Pereira, L. A. R. Batalha, A. O. Porto et al., "The influence of the R group in the thermal stability of $Sn_4R_4O_6$ (R = methyl, n-butyl or phenyl)," *Materials Research Bulletin*, vol. 38, no. 14, pp. 1805–1817, 2003.

[20] M. Nath and Sulaxna, "Di- and triorganotin(IV) derivatives of 5-amino-3H-1,3,4-thiadiazole-2-thione as precursors for SnS/SnO_2: thermal studies and related kinetic parameters," *Materials Research Bulletin*, vol. 41, no. 1, pp. 78–91, 2006.

[21] M. Nath, P. K. Saini, G. Eng, and X. Song, "Template synthesis and structural characterization of new diorganotin(IV) tetraazamacrocyclic complexes: precursors to produce pure phase nanosized SnO_2," *Journal of Coordination Chemistry*, vol. 62, supplement 22, p. 3629, 2009.

[22] M. Nath, P. K. Saini, G. Eng, and X. Song, "Synthesis and solid-state spectroscopic investigation of some novel diorganotin(IV) complexes of tetraazamacrocyclic ligands," *Journal of Organometallic Chemistry*, vol. 693, no. 13, pp. 2271–2278, 2008.

[23] H. P. Klug and L. E. Alexander, *X-Ray Diffraction Procedures for Polycrystalline and Amorphous Mater*, chapter 9, Wiley, New York, NY, USA, 2nd edition, 1974.

[24] H. H. Horowitz and G. Metzger, "A new analysis of thermogravimetric traces," *Analytical Chemistry*, vol. 35, no. 10, pp. 1464–1468, 1963.

[25] A. W. Coats and J. P. Redfern, "Kinetic parameters from thermogravimetric data," *Nature*, vol. 201, pp. 68–69, 1964.